Experimental generation and characterization of Devil's vortex-lenses

A. Calatayud, J. A. Rodrigo, L. Remón, W. D. Furlan, G. Cristóbal & J. A. Monsoriu

Applied Physics B
Lasers and Optics

ISSN 0946-2171
Volume 106
Number 4

Appl. Phys. B (2012) 106:915-919
DOI 10.1007/s00340-012-4913-0

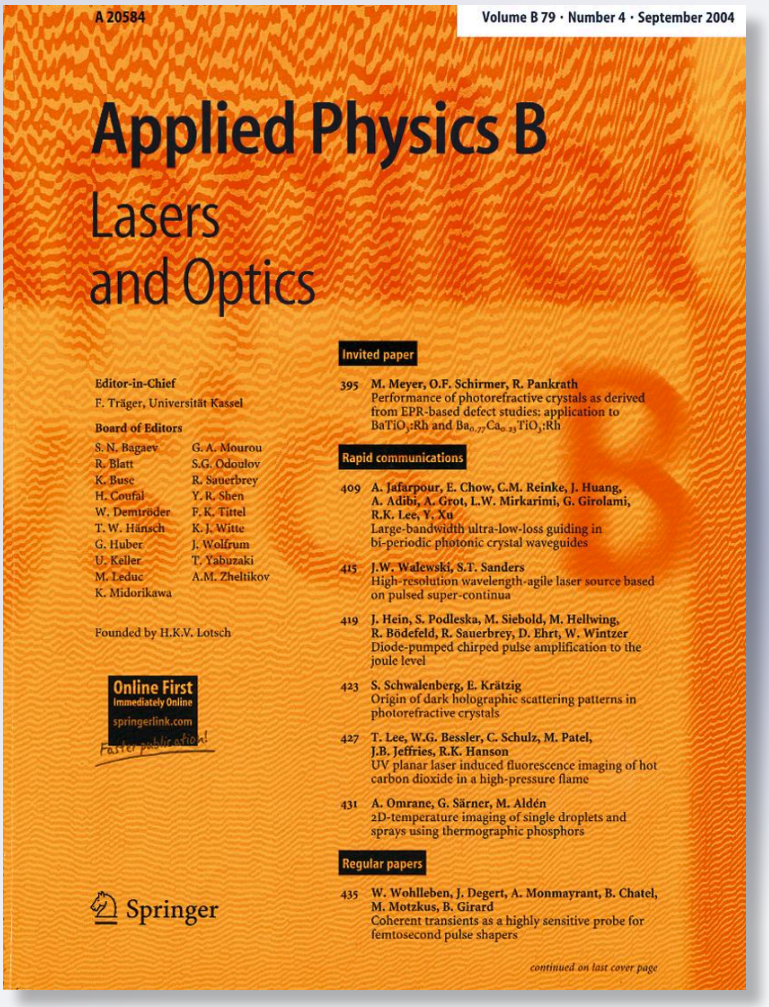

Springer

Appl Phys B (2012) 106:915–919
DOI 10.1007/s00340-012-4913-0

Applied Physics B
Lasers and Optics

Experimental generation and characterization of Devil's vortex-lenses

A. Calatayud · J.A. Rodrigo · L. Remón · W.D. Furlan · G. Cristóbal · J.A. Monsoriu

Received: 21 June 2011 / Revised version: 18 October 2011 / Published online: 24 February 2012

Abstract We propose the first experimental approach for both generation and characterization of high quality Devil's vortex-lenses. These new type of lenses, able to produce a sequence of optical vortices, are addressed onto a programmable spatial light modulator (SLM) operating in phase-only modulation. The static aberrations arising by the lack of flatness of the SLM display are characterized and mostly compensated by using a Shack–Hartmann wavefront sensor. The analysis of the residual aberrations and their effect on the vortex-lens performance are studied.

1 Introduction

Vortex lenses produce wavefronts with helical structure and zero axial intensity [1]. These optical vortices are special optical traps having the ability to set the trapped particles into rotation due to the orbital angular momentum of light [2, 3]. The most common solution adopted to produce optical vortices are spiral phase plates [4, 5]. Inspired in fractal zone plates [6, 7] and in the Devil's lenses [8], a new type of high efficient spiral fractal zone plates, the "Devil's Vortex-Lenses" (DVLs) [9] have been recently proposed to generate a sequence of focused optical vortices. A DVL is designed using the "Devil's staircase" or Cantor function, the distribution of the surface grooves in it producing a single main fractal focus composed of a sequence of discrete vortices. It was suggested [10] that the particular focal volume provided by DVLs could be profited as versatile and very efficient optical tweezers since, in optical trapping applications, in addition to rotating the trapped high index particles, the low-index particles can be trapped at center of the vortex. The relative angular velocity of the particles at the different traps can be modified by a parameter known as the topological charge, while the distances between the vortices can be modified by using different levels of the Cantor function.

In this paper DVLs are experimentally implemented in a programmable spatial light modulator (SLM). In order to observe the predicted focusing properties of different DVLs, an SLM operating in phase-only modulation was employed. In the experiment, the static aberrations arising from the proposed setup, mainly caused by the lack of flatness of the SLM display, are characterized and mostly compensated by using a Shack–Hartmann wavefront sensor. The effect of the residual aberrations in the vortex-lens performance is studied computing the intensity distribution along the optical axis and the transverse diffraction patterns along the propagation direction.

A. Calatayud · L. Remón · J.A. Monsoriu (✉)
Centro de Tecnologías Físicas, Universitat Politècnica de València, 46022 Valencia, Spain
e-mail: jmonsori@fis.upv.es

J.A. Rodrigo · G. Cristóbal
Instituto de Óptica, CSIC, Serrano 121, 28006 Madrid, Spain

W.D. Furlan
Departamento de Óptica, Universitat de València, 46100 Burjassot, Spain

2 Devil's vortex lenses

The design of a DVL [9] is based on the 1-D Cantor function [11], defined in the domain [0, 1] as:

$$F_S(x) = \begin{cases} \frac{l}{2^S} & \text{if } p_{s,l} \le x \le q_{s,l} \\ \frac{1}{2^S}\frac{x-q_{S,l}}{p_{S,l+1}-q_{S,l}} + \frac{l}{2^S} & \text{if } q_{s,l} \le x \le p_{s,l+1}, \end{cases} \quad (1)$$

being $F_S(0) = 0$ and $F_S(1) = 1$. This function takes the constant values $l/2^S$ in the intervals $p_{s,l} \le x \le q_{s,l}$ (with

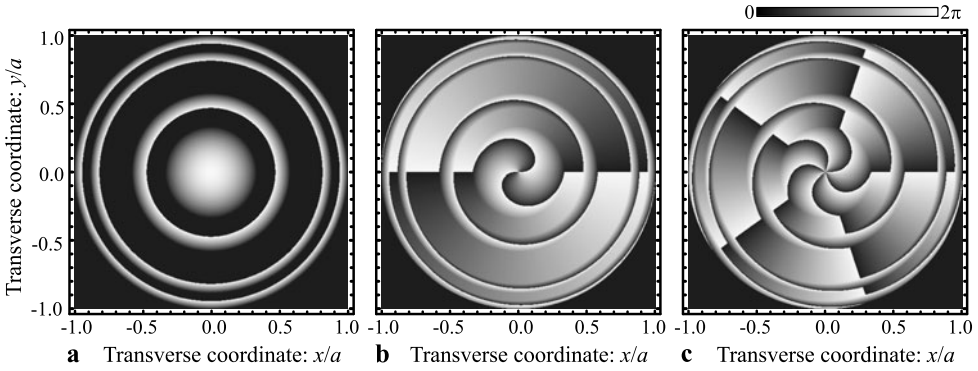

Fig. 1 (**a**) Phase variation as gray levels for a DVLs ($S = 2$) with different topological charges (**a**) $m = 0$, (**b**) $m = 2$, and (**c**) $m = 5$

$l = 1, \ldots, 2^S - 1$) defined by the gaps of the Cantor set generated at stage S, whereas in-between these intervals the function increases linearly. For example, for $S = 2$ the Cantor set has $2^S = 4$ segments of length $1/3^S = 1/9$ and $2^S - 1 = 3$ gaps located at the intervals $[1/9,\ 2/9]$, $[3/9,\ 6/9]$, $[7/9,\ 8/9]$, where $F_2(x)$ takes the constant values $1/4$; $2/4$ and $3/4$, respectively. From a particular $F_S(x)$ a DVL is designed as a pure-phase diffractive optical element with a transmittance defined, in polar coordinates, as:

$$q(r,\theta) = \exp\left[-i2^{S+1}\pi F_S\left(r^2/a^2\right)\right] \times \exp[im\theta], \qquad (2)$$

where a is the lens radius and m is the topological charge. Thus the transmittance of a DVL can be expressed as the product of two factors: the first one, associated with a Devil's lens [8], has only a radial dependence with a fractal structure along the squared radial coordinate; and the other one, corresponding to a vortex lens, has a linear phase dependence on the azimuthal angle. The form of DVLs for several values of the topological charge $m = 0$, 2, 5 are depicted in Fig. 1 in which the gray levels show the continuous phase variation.

3 Experimental setup and its characterization

To implement the proposed lenses we use a programmable SLM operating in phase-only modulation [12]. Specifically, we use a LCoS-SLM (Holoeye PLUTO, 8-bit gray-level, pixel pitch $d = 8$ μm and 1920×1080 pixels) calibrated for a 2π phase-shift at $\lambda = 633$ nm. In order to avoid efficiency degradation due to high time-fluctuations of the displayed phase, we addressed the so-called "5-5(543)" electrical signal scheme provided by the SLM manufacturer. This configuration gives better efficiency of the displayed phase even for phase-shift shorter than 2π, as demonstrated in [13]. Notice that, according to the data provided by the manufacturer, the diffraction efficiency of such a SLM is more than 80% of the light reflected by the display, which has a reflectivity about 60%. Therefore a total light efficiency about 50% can be reached.

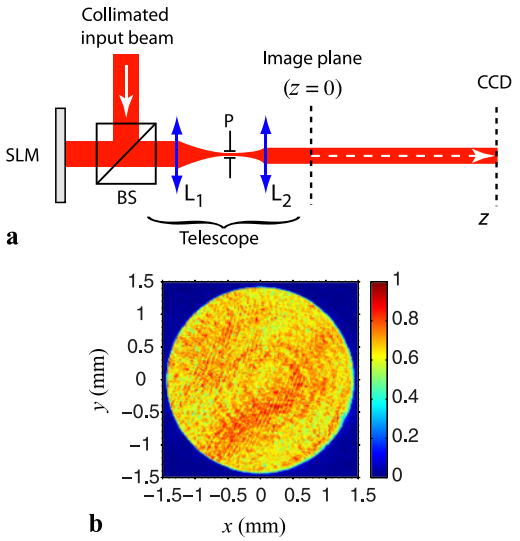

Fig. 2 (**a**) Experimental setup for implementing the proposed DVLs by means of a reflective *SLM*, which modulates a collimated laser beam at $\lambda = 633$ nm. The focal length of the relay lenses is set at $f_1 = 20$ cm and $f_2 = 10$ cm to obtain a telescopic magnification $0.5\times$. P is a pinhole used for spatial filtering of the signal, at the Fourier plane of L_1. The signal is addressed into a circular area of diameter 5.6 mm of the *SLM* display, which is imaged (**b**) at the output plane ($z = 0$) of the system

In Fig. 2(a) the experimental setup is sketched, where a 4-f setup (telescope) is used for spatial filtering of the signal. Such a filtering process is achieved by implementing a linear carrier phase $\varphi_c = \pi(x + y)/2d$, added to the lens modulation function $\psi(x, y) = \phi + \varphi_c \bmod 2\pi$, where $\phi = \arg[q(r,\theta)]$. Thus the addressed signal is guided into the first diffraction-order term in the Fourier plane of the first relay lens, L_1. This allows to isolate the signal from noise due to the unmodulated light (zero diffraction order) as well as the one corresponding to higher diffraction orders caused by the pixelated structure of the SLM display.

The generated signal can be also degraded by the lack of flatness of the SLM display and other static aberrations caused by the relay lenses, as collimation of the beam, etc. Several strategies to characterize and compensate the wavefront distortion caused by the SLMs have been recently re-

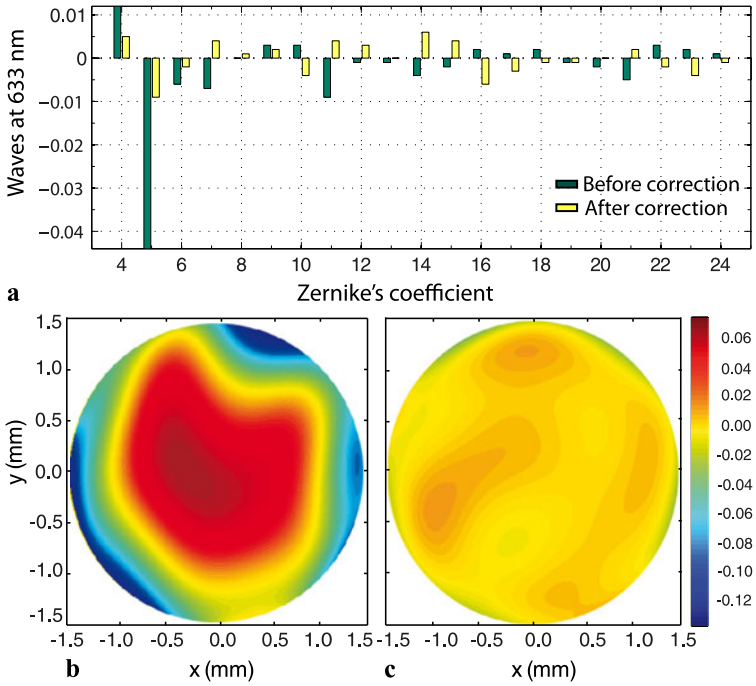

Fig. 3 (**a**) Zernike's coefficients corresponding to the retrieved phase distribution before and after performing the wavefront correction using the SLM: (**b**) and (**c**), respectively. Scale bar in waves at 633 nm

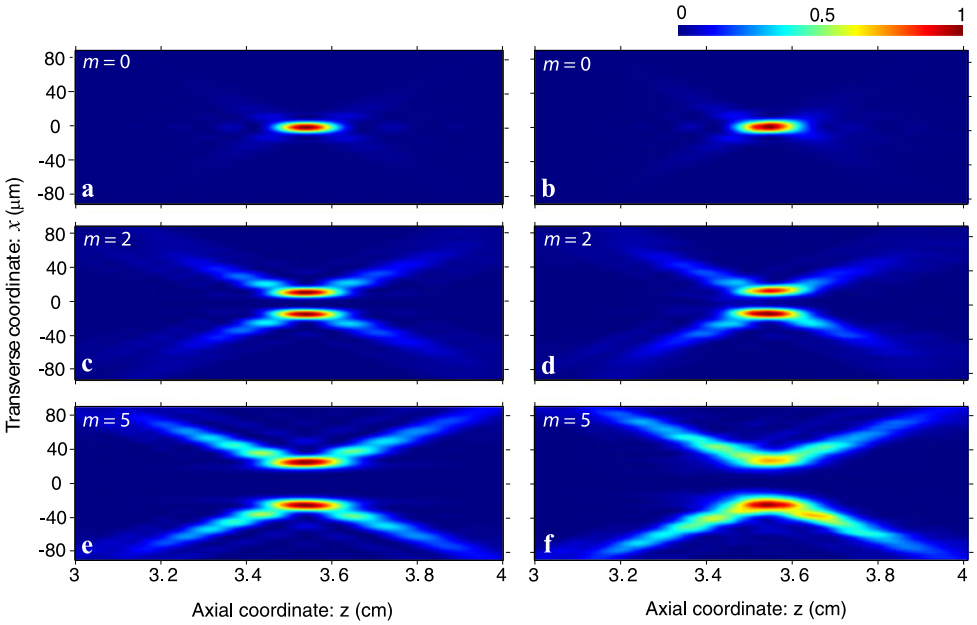

Fig. 4 Numerical (*left column*) and experimental (*right column*) irradiance obtained for vortex-lenses for different topological charges

ported, see [14, 15] and references therein. In this work we use a Shack–Hartmann (SH) wavefront sensor to characterize such aberrations, as proposed in [14]. In our case, the SH sensor has an aperture size of 5.95 mm × 4.76 mm and 39 × 31 micro-lenses (Thorlabs WFS150-7AR). Notice that the signal $\psi(x, y)$ is addressed into a circular area of diameter 5.6 mm of the SLM display, which is imaged into the SH sensor (placed at $z = 0$) by using a telescope with magnification 0.5× as depicted in Fig. 2(a). The SH allows analyzing the wavefront distortion present in the beam for $\phi = 0$, whose intensity distribution is shown in Fig. 2(b), in terms of the Zernike's orthogonal polynomials [16, 17]. These polynomials characterize the aberration terms of the retrieved phase $\phi_{ab}(x, y)$ at $z = 0$. Therefore the wavefront distortion can be compensated by addressing the complex conjugate of the retrieved phase as: $\psi(x, y) = \phi + \varphi_c - \phi_{ab}$ mod 2π. In our case, we considered the first 66 Zernike's coefficients for analyzing the retrieved phase (although in Fig. 3(a) only the predominant coefficients are represented). In the first measurement displayed in Fig. 3(b), the predominant aberrations are astigmatism at 45° and defocus with a coefficient (waves at $\lambda = 633$ nm) of 0.012λ and -0.044λ,

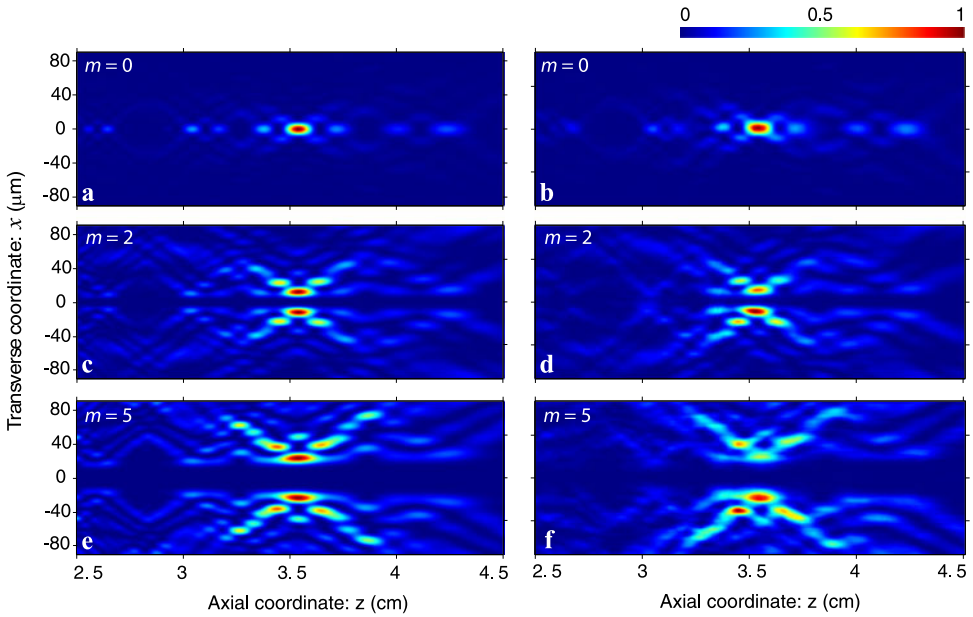

Fig. 5 Numerical (*left column*) and experimental (*right column*) irradiance obtained for DVLs for different topological charges

correspondingly. After implementing the wavefront correction, the aberration is partially compensated. Therefore we iteratively perform this process until maximum compensation of the aberration is reached. Indeed, after five iterations the initial wavefront distortion displayed in Fig. 3(b) is mostly compensated, see Fig. 3(c), except for low residual astigmatism at 45° (-0.006λ), defocus (0.01λ), spherical aberration (0.007λ) and secondary coma (-0.007λ), see yellow bars in Fig. 3(a) as well. The deviation of flatness of the wavefront is compensated from 0.09λ to 0.02λ RMS (root-mean-square error) with a peak-to-valley (PV) value of 0.06λ. Notice that the collimated input beam [Fig. 2(a)] was previously tuned using the SH sensor until obtaining a minimum deviation-flatness value of 0.03λ RMS and 0.11λ PV.

We underline that the 4-f setup is suitable for generating DVLs with different focal lengths by using an appropriate telescope-scaling factor $M = f_2/f_1$. To generate a sequence of optical vortices, we use a lens design given by (2). Specifically, for the considered scaling factor $M = 0.5$, the generated lenses have a pupil radius of $a = 1$ mm and the main focus is obtained at $z = 3.54$ cm.

In Fig. 4 the numerically computed irradiance (see Ref. [9] for further details) and the experimental one, corresponding to a conventional kinoform vortex-lens, are displayed for several values of the topological charge m [1]. As can be seen, the experimental results are in good agreement with the theoretical predictions. This fact demonstrates that the residual aberration does not significantly degrade the lens behavior. In our case, the irradiance was experimentally measured using a motorized stage in which the CCD camera (8-bit gray-level, pixel pitch of 3.6 μm and 1280×1024 pixels) was mounted. To correctly sample the diffracted field, we used a tube lens microscope ($10\times$ Zeiss Plan-Apochromat objective) attached to the CCD camera.

Unlike conventional kinoform vortex-lens, the irradiance for $m = 0$ produced by a DVL presents a main focus and subsidiary focal points surrounding it, yielding a focal volume with a characteristic fractal profile, see Figs. 5(a) and 6(a). This fractal behavior is also observed for different topological charges m, as can be seen in Fig. 5. The small deviation between numerical and experimental data close the main focal region is caused by the residual astigmatism and coma aberrations of the SLM as well as other aberrations arising from the microscope objective [18]. Nevertheless, a well-defined vortex structure is obtained as is observed in Fig. 6(b).

4 Conclusions

The focusing properties of Devil's vortex-lenses have been experimentally analyzed for the first time in the literature. These lenses have been encoded onto an SLM operating in phase-only modulation with compensated aberrations. The good performance of the experimental setup is confirmed by the comparison between the experimental values of the irradiance along the optical axis and the theoretical predictions. It has been demonstrated that for multiple-plane optical trappings, the DVL can generate a light beam with axially distributed optical vortices. The transverse patterns appearing along the propagation distance present several concatenated doughnut modes. The particular focal volume provided by DVLs could be profited as versatile and efficient multiple-plane optical trap in the microscopic scale. Another potential application of DVL arises in X-ray microscopy [19] where

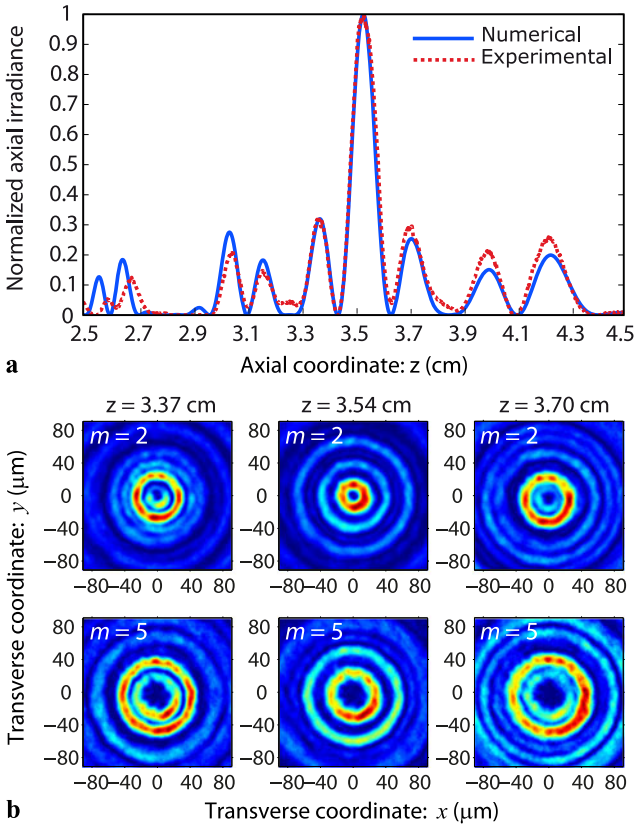

Fig. 6 (**a**) Numerical and experimental axial irradiance obtained for a DVL with $m = 0$. (**b**) Transverse diffraction patterns at several propagation distances z corresponding to the Devil's vortex-lens with topological charges $m = 2$ and 5

the azimuthal component of the DVL acts as a Hilbert phase filter that can be used for detecting the phase component of objects with complex index of refraction. In the case of biological specimens, the additional phase sensitivity can provide enhanced contrast. Additionally, the multifocal nature of the lens, resulting from its fractal structure along the radial coordinate, could provide a high depth of field, especially with wideband sources [8, 10].

Acknowledgements The financial support of the Spanish Ministry of Science and Innovation under projects DPI2008-02953, TRA2009-0215 and TEC2010-20307 is acknowledged. We also acknowledge the support from Generalitat Valenciana through the project PROMETEO2009-077. J.A.R. gratefully acknowledges a "Juan de la Cierva" grant and the financial assistance provided by the Universitat Politècnica de València (grants PAID-02-10 and PAID–5-11). L.R. acknowledges a fellowship of "Fundación Cajamurcia", Spain.

References

1. K. Crabtree, J.A. Davis, I. Moreno, Appl. Opt. **43**, 1360 (2004)
2. F.S. Roux, Opt. Commun. **242**, 45 (2004)
3. G. Gbur, T.D. Visser, Opt. Commun. **259**, 428 (2006)
4. W.M. Lee, X.-C. Yuan, W.C. Cheong, Opt. Lett. **29**, 1796 (2004)
5. S.H. Tao, X.-C. Yuan, J. Lin, R. Burge, Appl. Phys. Lett. **89**, 031105 (2006)
6. G. Saavedra, W.D. Furlan, J.A. Monsoriu, Opt. Lett. **28**, 971 (2003)
7. J.A. Rodrigo, T. Alieva, M.L. Calvo, J.A. Davis, J. Mod. Opt. **52**, 2771 (2005)
8. J.A. Monsoriu, W.D. Furlan, G. Saavedra, F. Giménez, Opt. Express **15**, 13858 (2007)
9. W.D. Furlan, F. Giménez, A. Calatayud, J.A. Monsoriu, Opt. Express **17**, 21891 (2009)
10. W.D. Furlan, F. Giménez, A. Calatayud, L. Remon, J.A. Monsoriu, J. Eur. Opt. Soc., Rapid Publ. **5**, 10037s (2010)
11. D.R. Chalice, Am. Math. Mon. **98**, 255 (1991)
12. J.A. Davis, L. Ramirez, J.A.R. Martín-Romo, T. Alieva, M. Calvo, Opt. Lett. **29**, 1321 (2004)
13. A. Lizana, A. Márquez, L. Lobato, Y. Rodange, I. Moreno, C. Iemmi, J. Campos, Opt. Express **18**, 10581 (2010)
14. C. López-Quesada, J. Andilla, E. Martín-Badosa, Appl. Opt. **48**, 1084 (2009)
15. J.A. Rodrigo, T. Alieva, A. Cámara, O. Martínez-Matos, P. Cheben, M.L. Calvo, Opt. Express **19**, 6064 (2011)
16. R.J. Noll, J. Opt. Soc. Am. **66**, 207 (1976)
17. M. Born, E. Wolf, *Principles of Optics* (Cambridge University Press, Cambridge, 1999)
18. R.K. Singh, P. Senthilkumaran, K. Singh, J. Opt. A, Pure Appl. Opt. **10**, 075008 (2008)
19. A. Sakdinawat, Y. Liu, Opt. Lett. **32**, 2635 (2007)